The Inclusion of Fringing Capacitance and Inductance in FDTD for the Robust Accurate Treatment of Material Discontinuities

Chris J. Railton, *Member, IEEE*

***Abstract*—The analysis of structures, which contain sharp material discontinuities using the finite-difference time-domain method (but without resorting to a very fine mesh) although much researched, has not yet been definitively solved. In this paper, the fringing fields associated with the discontinuities are dealt with by adjusting the permittivity and permeability assigned to the field nodes that are immediately adjacent to the discontinuities. This method is shown to be effective for a variety of structures and to be without the problems of violating energy or divergence conservation.**

***Index Terms*—FDTD.**

I. Introduction

THE treatment of abrupt and often electrically small material discontinuities, such as thin wires, microstrips or printed circuit board (PCB) traces, in the finite-difference time-domain (FDTD) method has been the subject of research for a number of years. For instance, the treatment of thin wires and narrow microstrips, embedded in an FDTD mesh, have been treated in [1]–[9].

These have involved introducing static solutions either into the full three-dimensional (3-D) algorithm or into planar models. Of the full-wave approaches, some early attempts at solving the problem, while achieving good levels of efficiency and accuracy, were prone to late time instability. Later contributions successfully overcame the stability problem by ensuring reciprocal interaction between nodes, but local charge conservation was not guaranteed, and this limited the range of applications for the method.

In [10] a simple, effective, and robust technique, without these limitations, was investigated, in which the complicated field distribution around edges and wires is accounted for by modifying the permittivity and permeability assigned to the adjacent field nodes. In this paper, this method is improved with the use of more accurate and simpler empirical formulas, which are based on the physical properties of the FDTD mesh itself. This leads to a more robust method, which can be applied to a wide variety of discontinuity types with a consequential saving in computer resources. With the use of just a small precalculated lookup table, results at least as accurate as those obtained previously can be achieved, but now without the drawbacks of either late time instability or lack of local charge conservation.

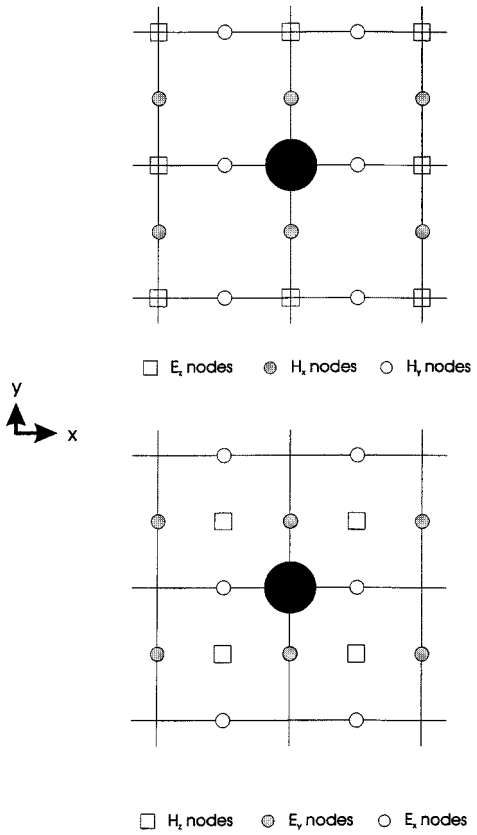

Fig. 1. Thin wire embedded in the FDTD mesh. (top) TM plane. (bottom) TE plane.

Although the method presented here is developed and demonstrated for the specific case of planar structures, the method can be used for a more general class of geometries including dielectric waveguide and planar waveguide junctions and other discontinuities.

II. Conductors of Small Cross Section in the FDTD Mesh

As an example, consider the case of a conducting wire above a ground plane. This structure can be viewed as a transmission

Manuscript received March 2, 2000; revised August 21, 2000.

The author is with the Faculty of Engineering, Centre for Communications Research, University of Bristol, Bristol BS8 1UB U.K. (e-mail: chris.railton@bristol.ac.uk).

Publisher Item Identifier S 0018-9480(00)10721-5.

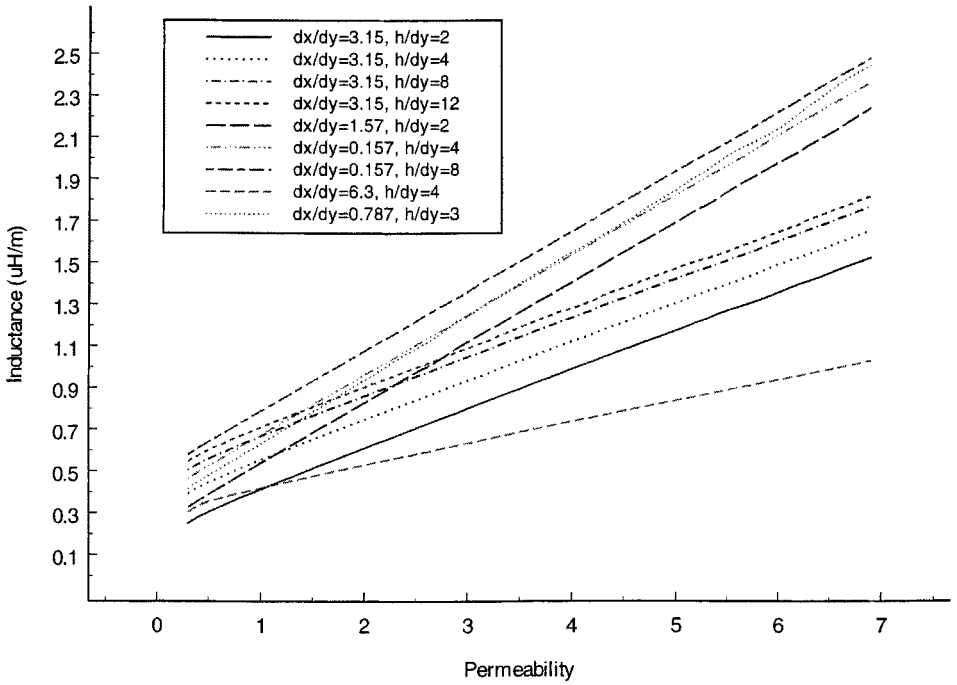

Fig. 2. Predicted inductance versus assigned permeability for various mesh sizes.

line that has a capacitance C and inductance L per unit length, which depends on the wire radius as follows [11]:

$$L = \frac{\mu}{\pi} \cosh^{-1}\left(\frac{h}{a}\right)$$
$$C = \frac{\pi\varepsilon}{\cosh^{-1}\left(\frac{h}{a}\right)}$$

where a is the radius of the wire and h is the height of the wire above the ground plane.

Similar equations exist, e.g., [12], from which the inductance and capacitance of a microstrip line or a PCB track can be calculated as a function of the geometry of the structure. Any planar transmission line can be treated using the method described here as long as the quasi-static transmission-line parameters are available.

In the standard FDTD mesh, the capacitance and inductance associated with the fringing fields that exist around the wire can be modeled by altering the permittivity associated with the transverse E-field nodes and the permeability associated with the transverse H-field nodes, respectively. If the wire is orientated along the z-axis, as shown in Fig. 1, the eight nodes that are at distances of $dx/2$ and $dy/2$ from the conductor are considered, where dx and dy are the cell size in the x- and y-directions, respectively. For a wider strip, the six nodes that are closest to each edge, but not on the strip itself, are considered (12 in total).

III. Obtaining the Empirical Mapping

In order to derive a mapping between the material parameters assigned to the FDTD nodes and the resulting predicted capacitance and inductance per unit length, a large number of runs were done on boxed microstrips with a variety of cell sizes, strip widths, and strip heights. The boxed structure was chosen in order to avoid any possible inaccuracies due to the effects of imperfect absorbing boundary conditions. For convenience the box cross section was chosen to 10 mm $\times$ 12.7 mm. Cell sizes between 0.1–2 mm and strip heights varying from 0.635–5.08 mm were used. Any convenient size could have been used and the same final results would be obtained.

For each geometry and mesh size, two runs were done using a two-dimensional version of the FDTD algorithm with the propagation constant set to 100. This value was chosen since, for the quasi-TEM mode of microstrip, the corresponding frequencies are low enough for dispersive effects to be small, but high enough to allow accurate results to be obtained with a moderate number of iterations. The structure was excited with a narrow current pulse between the ground plane and strip and the resulting field as a function of time was probed. A spectral analysis of the time sequence yields a series of peaks at frequencies where different modes propagate with the chosen propagation constant. The first peak gives the frequency for the quasi-TEM mode from which the phase velocity is calculated. A second run is then done, but this time, the discrete Fourier transform of the fields across the entire cross section of the structure is calculated at the frequency obtained in the first step. From this knowledge of the field distribution, the characteristic impedance of the microstrip is calculated by taking appropriate integrals of the electric and magnetic fields. With this information, the predicted inductance and capacitance per unit length is calculated.

Some example results are given in Fig. 2, which show the behavior of inductance versus assigned permeability for a narrow microstrip whose width is less than the cell size. Corresponding results showing the behavior of the capacitance versus assigned permittivity are given in Fig. 3. For the case where the strip is wider than a single cell, the behavior of the inductance versus assigned permeability is shown in Fig. 4. The form of each of these mappings and ways in which they can be approximated by simple formulas will now be discussed.

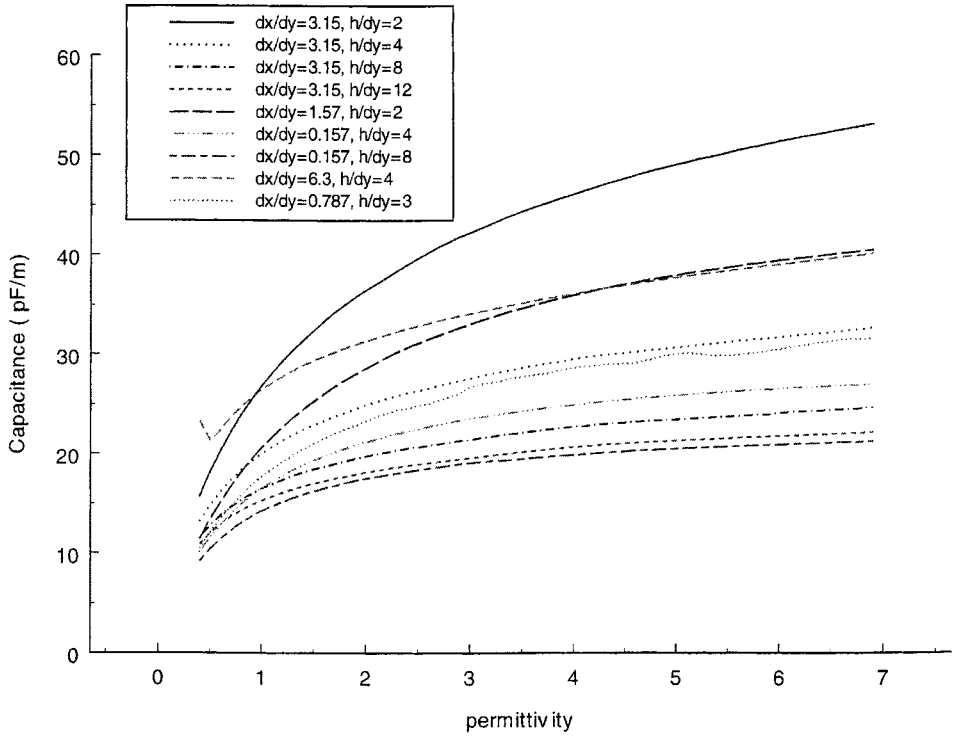

Fig. 3. Predicted capacitance versus assigned permittivity for various mesh sizes.

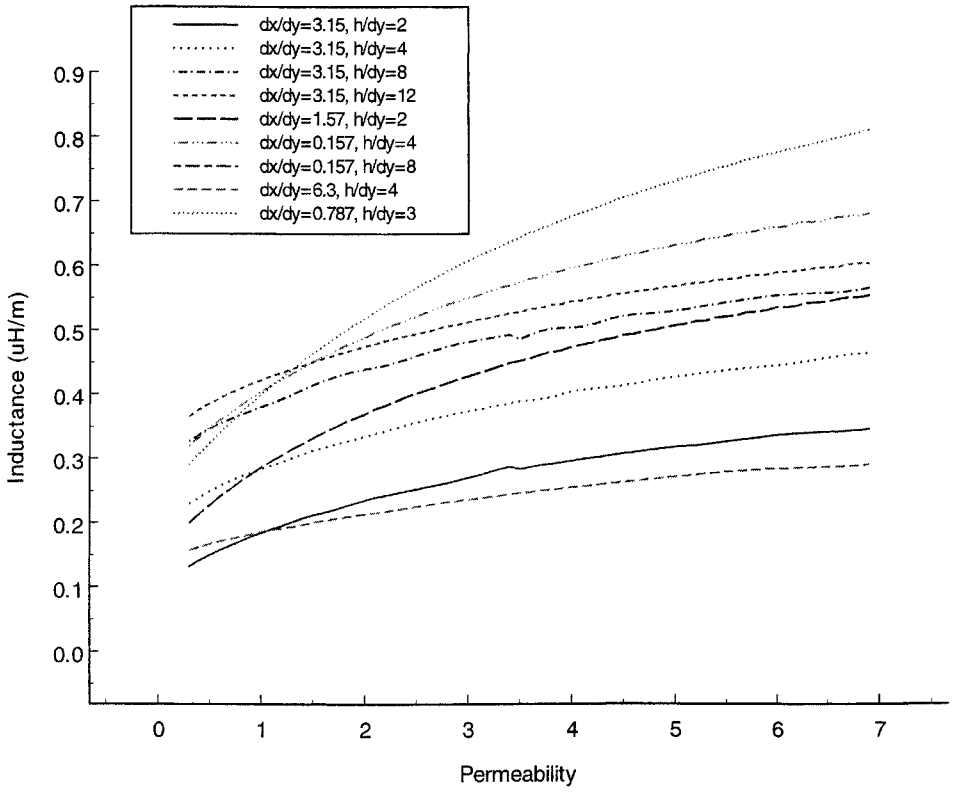

Fig. 4. Predicted inductance versus assigned permeability for various mesh sizes for wide strips.

IV. Fringing Field Inductance

For the example of a thin strip or wire where the four H-field nodes adjacent to the strip are affected, it is found that, in the limit of high permeability, the inductance of the wire is proportional to the permeability of the surrounding nodes. Moreover, the slope of the graphs is dependent only on the aspect ratio of the mesh and not on the height of the strip above the ground

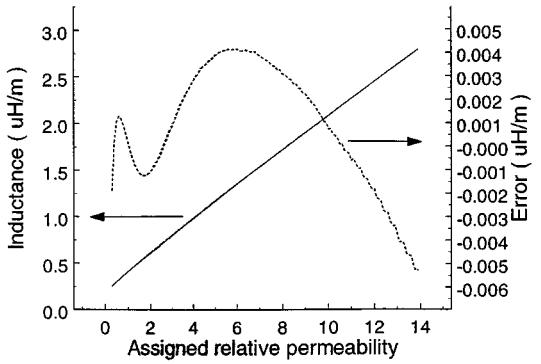

Fig. 5. Error in the approximate formula for L.

plane. Where the permeability is low and, in particular, if the permeability is less than that of the surrounding material, the dependence of inductance on the permeability of the surrounding material closely follows an exponential. Therefore, the inductance of the wire can be approximated by

$$L \approx (a\mu + b)(1 - k_1 e^{-k_2 \mu})$$

where L is predicted inductance of the strip under consideration and μ is the permeability assigned to the neighboring H-field nodes. a, b, k_1, and k_2 are parameters that are, at present, derived by curve fitting to the results obtained from the many FDTD runs.

If the discontinuity is part of a structure that spans a number of cells, such as a patch or a wider microstrip, then only the nodes adjacent to the discontinuity will be altered. In this case, the total inductance will be the combination of the inductance of the altered nodes and the inductance of the rest of the structure. In this case, it has been found that the inductance of the structure can be well approximated by

$$L \approx L_\infty - \frac{1}{(a\mu + b)(1 - k_1 e^{-k_2 \mu})}$$

where L_∞ is the asymptotic value of the inductance in the limit of infinite permeability.

An example of the typical accuracy of this approximation is given in Fig. 5. It can be seen that over most of the plotted range, the error is less than 0.1%.

V. Fringing Field Capacitance

The dependence of the capacitance of the wire on the permittivity of the modified cells is more complicated since it is a combination of the self capacitance of the wire, the capacitance between the wire and the ground plane, and the capacitance of the modified nodes. It has been found that the total capacitance of the wire can be approximated by a similar formula to that used to approximate the inductance of a wide strip

$$C \approx C_\infty - \frac{1}{(a\varepsilon + b)(1 - k_1 e^{-k_2 \varepsilon})}$$

where, as for the case of the inductance, the parameters in the equation are, at present, derived empirically by doing a number of FDTD runs on a test structure. Unlike the case of the inductance, the same approximation is effective for structures that

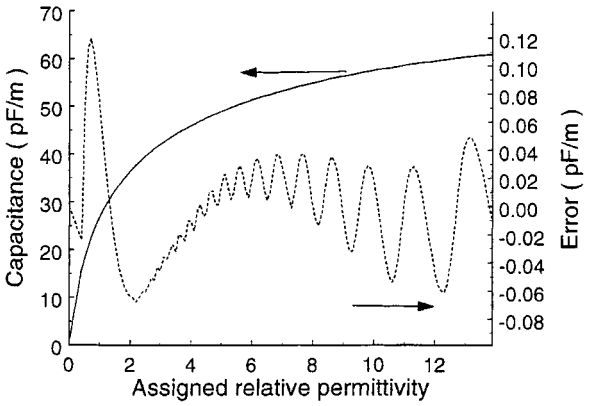

Fig. 6. Error in the approximate formula for C.

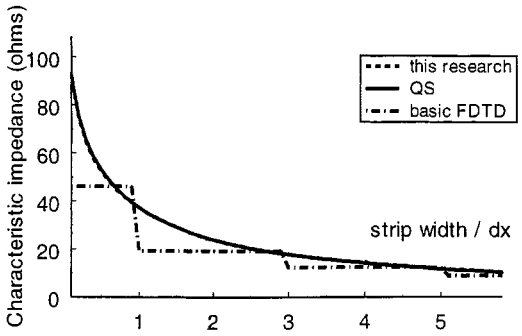

Fig. 7. Characteristic impedance of microstrip—substrate permittivity of 10.5.

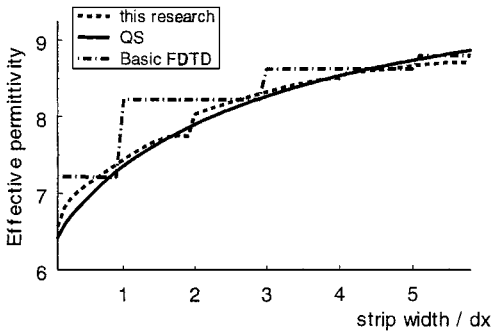

Fig. 8. Effective permittivity of microstrip—substrate permittivity of 10.5.

span many cells as well as those that are smaller than a single cell.

An example of the accuracy of this approximation is given in Fig. 6. It can be seen that, over the plotted range, the error is less than 0.1%.

VI. Application to Microstrip Lines

In order to discover the accuracy and effectiveness of this method, the characteristic impedances and effective permittivities of microstrip lines having widths varying from one-tenth of the cell size to eight times the cell size was calculated. Using, in this case, a lookup table consisting of just 30 precalculated numbers, the plots shown in Figs. 7–10 were derived. Here, the results obtained from this research are compared to the quasi-static formulas and to the unmodified FDTD. Clearly, in the latter case, the result only changes when the size of the strip

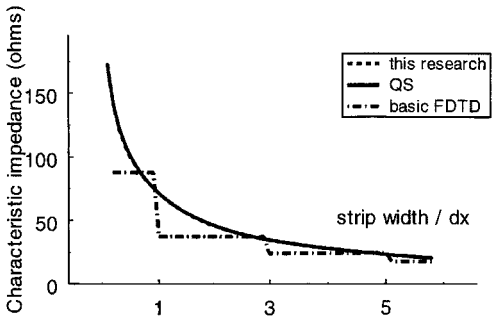

Fig. 9. Characteristic impedance of microstrip—substrate permittivity of 2.5.

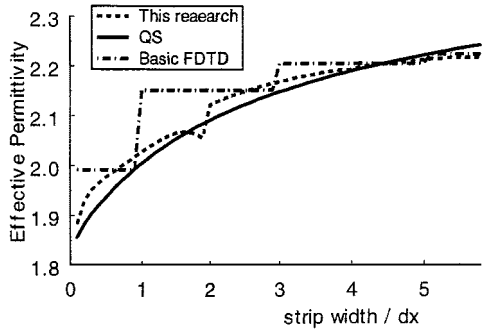

Fig. 10. Effective permittivity of microstrip—substrate permittivity of 2.5.

approximates to a different multiple of cell size. For this test, the strip was in the x–z-plane with z being the direction of propagation. The substrate height was 0.635 mm, $dx = 1$ mm, $dy = 0.3175$ mm, and $dz = 1$ mm. The width of the strip was chosen to be between 0.1–6 mm and the frequency was approximately 1 GHz. The structure was contained in a box of cross-sectional dimensions 12.7 mm $\times$ 10 mm. It can be seen that the agreement between the results obtained using this research and [12] are, for the characteristic impedance, excellent, and for the effective permittivity, very good. In both cases, the improvement over the standard FDTD is considerable.

It is to be noted that the same lookup table can be used for a substrate of any permittivity. This is to be expected since the singular behavior of the fields near sharp discontinuities is not affected by the substrate.

Results for the effective permittivity as a function of frequency for six different microstrip lines are shown in Figs. 11 and 12. Here, it can be seen that the results predicted by the modified FDTD method follow closely those calculated using the well-established spectral domain method apart from a small offset. That the modifications to the material parameters, which are based on quasi-static considerations, cause improvements over a frequency range where the nonstatic nature of the field is significant reflects the fact that the geometrical features that are being accounted for are electrically small.

VII. Application to Larger Planar Structures

In the foregoing, separate empirical formulas were derived for the case of strips that are narrower than a cell size, for cases where the strip width was between dx and $2dx$, and again for wider strips where the width was between $3dx$ and $4dx$. In each of these cases, the nodes most closely adjacent to the edges are

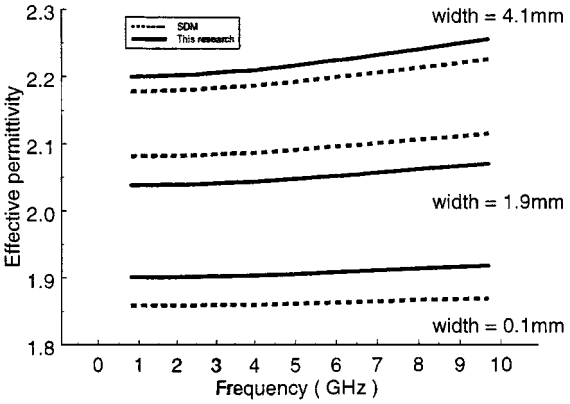

Fig. 11. Dispersion curves for three different microstrips. Substrate permittivity is 2.5.

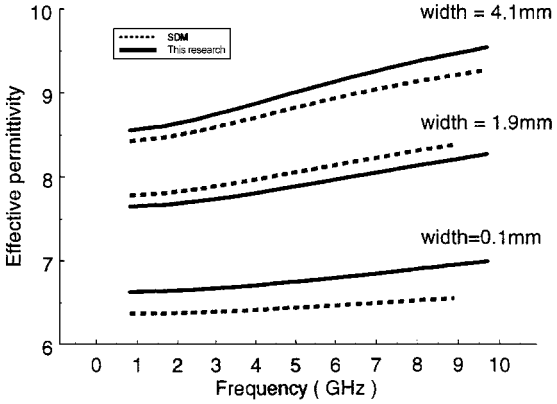

Fig. 12. Dispersion curves for three different microstrips. Substrate permittivity is 10.5.

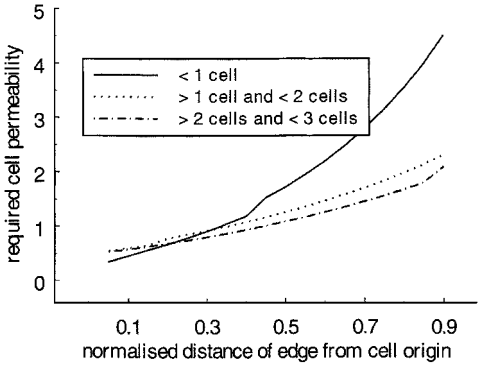

Fig. 13. Required permeability as a function of edge position relative to the cell.

modified. It would be expected, however, once the metal strip was wide enough such that the two edges did not significantly interact, that the assigned material parameters would depend only on the position of the individual edge relative to the cell and not on the strip width. The graphs shown in Figs. 13 and 14 demonstrate that this is indeed the case. In these figures, the required value of the modified permittivity and permeability is given for an edge as a function of its position relative to the cell. The x-axis gives the position of the edge normalized to the size of the cell and the three plots show results for the cases where the entire strip covers different numbers of cells. It can

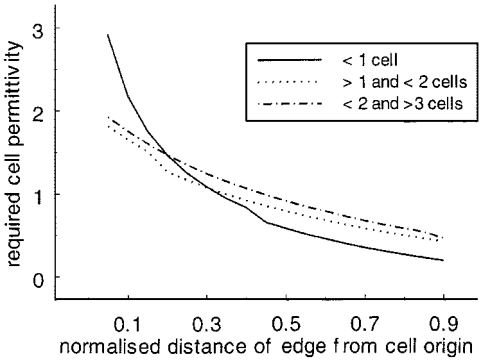

Fig. 14. Required permittivity as a function of edge position relative to the cell.

be seen that, for the wider strips, the required modifications to the material parameters are similar regardless of the number of cells covered by the strip. Thus, these formulas can be used for arbitrarily large strips and patches to compensate for the effects of the edge singularities.

VIII. Conclusion

In this paper, a procedure has been described whereby simple analytical formulas can be derived and incorporated in the FDTD algorithm, which allow the accurate treatment of wires and microstrip structures without either having to resort to a very fine mesh or to risk introducing spurious divergence or late time instability. The resulting scheme is simple, versatile, robust, and readily capable of extension to more complex incidences of electrically small structures such as microstrip steps, junctions, and bends.

References

[1] R. Holland and L. Simpson, "Finite difference analysis of EMP coupling to thin struts and wires," in *IEEE Trans. Electromagn. Compat.*, vol. EMC-23, May 1981, pp. 88–97.

[2] A. Taflove and K. Umashankar, "The finite-difference time-domain method for numerical modeling of electromagnetic wave interactions," *Electromagnetics*, vol. 10, pp. 105–126, 1990.

[3] C. J. Railton, "The simple, rigorous and effective treatment of thin wires and slots in the FDTD method," in *24th European Microwave Conf.*, Cannes, France, 1994, pp. 1541–1546.

[4] J. Grando, F. Issac, M. Lemistre, and J. C. Alliot, "Stability analysis including wires of arbitrary radius in FD-TD code," in *IEEE AP-S Symp. Dig.*, Ann Arbor, MI, 1993, pp. 18–21.

[5] P. Bonnet, X. Ferrieres, J. Grando, and J. C. Alliot, "FVTD applied to dielectric or wire structures," in *IEEE AP-S Symp. Dig.*, Baltimore, MD, 1996, pp. 2126–2129.

[6] D. B. Shorthouse and C. J. Railton, "Incorporation of static field solutions into the finite difference time domain algorithm," *IEEE Trans. Microwave Theory Tech.*, vol. 40, pp. 986–994, May 1992.

[7] C. J. Railton, D. B. Shorthouse, and J. P. McGeehan, "The analysis of narrow microstrip lines using the finite difference time domain method," *Electron. Lett.*, pp. 1168–1170, 1992.

[8] J. Craddock and C. J. Railton, "Stable inclusion of *a priori* knowledge of field behavior in the FDTD algorithm: Application to the analysis of microstrip lines," in *IEEE AP-S Symp. Dig.*, Baltimore, MD, 1996, pp. 1300–1303.

[9] W. K. Gwarek, "Analysis of arbitrarily-shaped planar circuits—A time domain approach," *IEEE Trans. Microwave Theory Tech.*, vol. MTT-33, pp. 1067–1072, Oct. 1985.

[10] C. J. Railton, "An investigation into the properties of the FDTD mesh with application to wires and strips," *Int. J. Numer. Modeling*, pp. 69–79, Apr. 1999.

[11] D. Pozar, *Microwave Engineering*. New York: Wiley, 1998.

[12] A. Balanis, *Advanced Engineering Electromagnetics*. New York: Wiley, 1989.

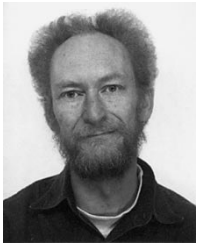

Chris J. Railton (M'88) received the B.Sc. degree in physics with electronics from the University of London, London, U.K., in 1974 and the Ph.D. degree in electronic engineering from the University of Bath, Bath, U.K., in 1988.

From 1974 to 1984, he was with the Scientific Civil Service, during which time he was involved with a number of research and development projects in the areas of communications, signal processing and electromagnetic compatibility (EMC). From 1984 and 1987, he was with the University of Bath, where he was involved with mathematical modeling of boxed microstrip circuits. He is currently with the Centre for Communications Research, University of Bristol, Bristol, U.K., where he leads the Computational Electromagnetics Group, which is involved in the development of new algorithms and their application to monolithic microwave integrated circuits (MMICs), planar antennas, optical waveguides, microwave and RF heating, EMC, and high-speed logic.